

Design Optimization and Improvement of 6S-10P Outer-Rotor AICiRaF PMFSM using Finite Element Analysis

**Mohamed Hariz Mohammed Thayir¹, Mahyuzie Jenal^{1*},
RoZIAH Aziz¹, Erwan Sulaiman¹, Md Zarafi Ahmad¹**

¹Faculty of Electrical and Electronic Engineering,
Universiti Tun Hussein Onn Malaysia, Parit Raja, Batu Pahat, 86400, MALAYSIA

*Corresponding Author Designation

DOI: <https://doi.org/10.30880/eeee.2021.02.01.008>
Received 02 March 2021; Accepted 06 April 2021; Available online 30 April 2021

Abstract: Alternate circumferential and radial flux (AICiRaF) is a new proposed design in permanent magnet flux switching machine (PMFSM). Even though AICiRaF PMFSM offers high torque and power density, it is however produces high cogging torque compared to other types of FSM. To deal with this problem, continuous research and development on electric machines should be applied to improve the cogging torque drawback. In this study, 6 slots 10 pole AICiRaF PMFSM by employing outer rotor, E core shape of armature coil, permanent magnet in radial and circumferential shape is to study and compare the performance of initial outer rotor design and optimized outer rotor design in the term of torque performances. The optimized design has be evaluated by varying eight types of main parameters to observe which design gives better output torque. Initially, design procedures of AICiRaF PMFSM including parts drawing, material and condition setting, the properties setting are all explained. Then, coil arrangement test is conducted to perform 3 phase armature coil arrangement. Then, no-load analysis is conducted to analyse cogging torque, flux linkage, flux distribution and back-EMF of motor followed by load analysis which analyses the torque speed characteristics and output power of the motor. No-load analysis and load analysis are conducted using finite element analysis of JMAG Designer 16.1. Subsequently, the best parameters for all main parts have been obtained and undergone certain examinations before finally summarized at the end of study.

Keywords: AICiRaF PMFSM, Optimization, Outer Rotor

1. Introduction

Permanent magnet transition exchanging machine (PMTEM) is a joint endeavor of switch reluctant machine (SRM) and permanent magnet synchronous machine (PMSM). The principle of this particular machine was presented as a solitary stage attenuation in 1955 by Rauch and Johnson. At that point, it evolves tremendously until 1997 whereby the initial three-stage engine was created by E. Hoang [1].

On the other hand, flux switching machine (FSM) is likewise a kind of synchronous engine. It has the benefits of high torque yield capacity, high proficiency, solid irreversible demagnetization withstands ability, great warm dispersal and fluid cooling conditions, and ideal rapid task. These favorable circumstances are important for electric drive frameworks, for example, electric vehicles and cross breed electric vehicles [2].

However, most of the researches are mainly focused on inner-rotor FSMs configurations [3-7]. A latest report on outer-rotor PMFSM has been invented in 2010 with the target output for light weight electric vehicle (EV) applications. Nonetheless, with constant PM flux as the only excitation flux source, it suffers with demagnetization effect, flux leakage to the shaft, unavailability torque production for heavy duty application and hard to control PM flux. In addition, with V-core segmented stator structure, the manufacturing and assembling process also become difficult [8-12].

In order to overcome this drawbacks, a new structure of outer-rotor AICiRaF PMFSM is proposed and optimized. The presence of alternate arrangement of rare-earth permanent magnet makes the machine becomes more attractive especially on modulating PM flux as well as high possibility to improve maximum torque and power densities. Figure 1 shows various topologies of outer-rotor flux switching machine (FSM) and Figure 2 depicts proposed 6S-10P outer-rotor AICiRaF PMFSM (initial).

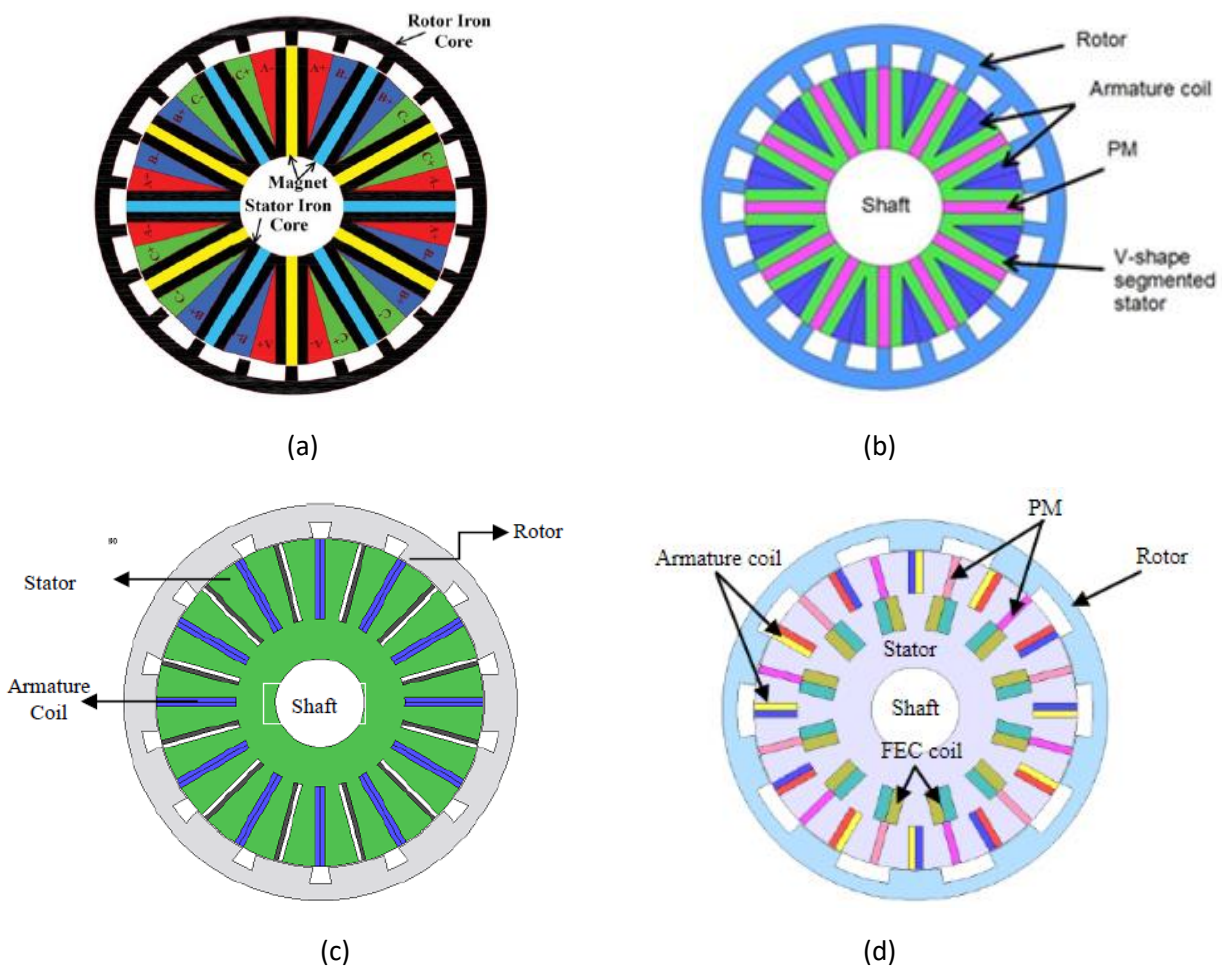


Figure 1: Various topologies of outer-rotor flux switching machine (FSM) (a) 12S-22P PMFSM (b) 12S-24P V-shape segmented stator PMFSM (c) 12S-14P field-excitation FSM (d) 12S-14P hybrid excitation FSM

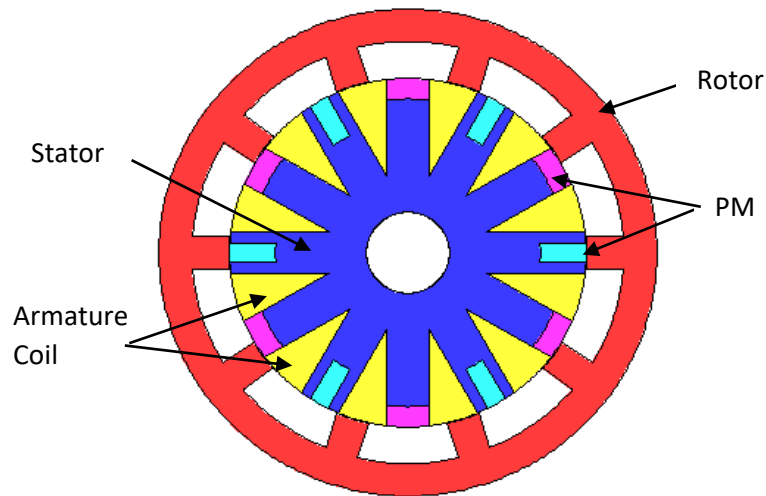


Figure 2: Proposed 6S-10P outer-rotor AlCiRaF PMFSM (initial)

2. Materials and Methods

The fundamental feature of JMAG-Designer is mainly about the process of geometry sketching, model setting such as material used, condition setting, circuit, study magnetic, run analysis, mesh and plot the graph of result. Additionally, JMAG Designer has simplify the research in the aspect of cost and time as the result out of the simulation is reliable and possible. JMAG Designer also precisely catch and rapidly assess complex physical phenomena inside the machine itself.

2.1 Materials and conditions

Table 1 depicts components and condition applied while setting up for rotor, stator, armature coil and permanent magnet where for the rotation of rotor, the durable revolution speed is set to 500 r/min. Furthermore, the nodal force is additionally applied with upward direction on rotation axis. The reason is to specify and calculate the torque acting on magnetic materials.

Table 1: List of specific materials and conditions

Parts	Materials	Condition
Rotor	Nippon Steel 35H210	Motion: rotation Torque: nodal force
Stator	Nippon Steel 35H210	-
Armature Coil	Conductor Copper	FEM Coil
Permanent Magnet	Neomax35AH (irreversible) (Alternate Radial and Circumferential Anisotropic Pattern)	Motion: rotation Torque: nodal force

2.2 Methods

In general, this study is divided into two parts specifically geometry editorial manager and JMAG-Designer. Geometry editorial manager is used to figure out every piece of machine separately, for example, stator, rotor, armature coil, and FEC while the condition settings and simulation must be made using JMAG-Designer. The flowcharts for the geometry editor and JMAG-Designer are shown in Figure 3.

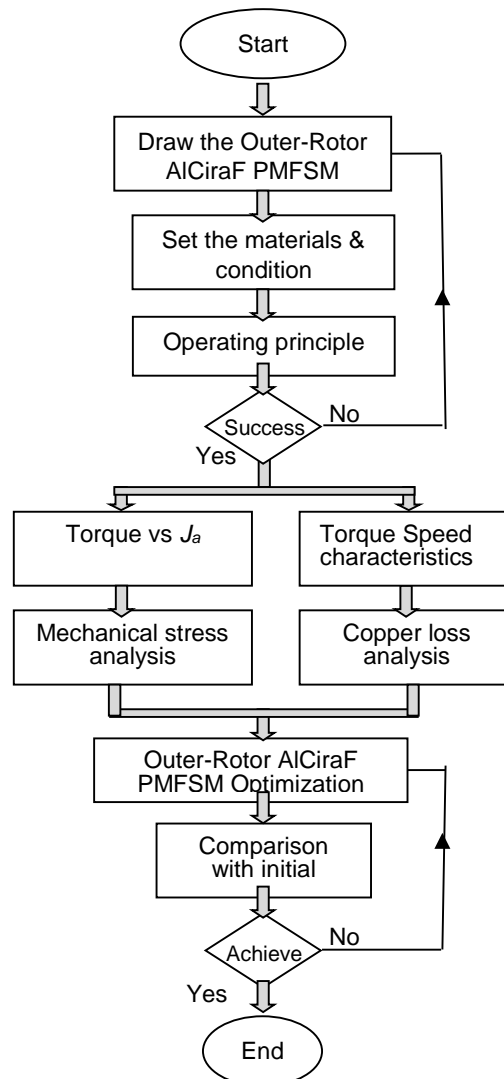


Figure 3: Overall project flowchart

2.3 Design topologies and specifications

2.3.1 Permanent magnet design

This step is to fill up the compartment of machine after done with designing the stator, rotor and armature coil. For nine design, the stack length value was constant which is 70mm^2 . Density of magnet was set to 7550 kg/m^3 section has two types of pattern of permanent magnet which is Radial and Circumferential. In addition, the material of magnet that used is Neomax-35AH (irreversible) that contains density of 7550kg/m^3 . By using density formula that shows in Eq. 1.

$$\rho = \frac{\text{mass of PM}}{\text{volume of PM}} \quad \text{Eq. 1}$$

where

ρ = Density of magnet (7550 kg/m³)
 mass = 0.5 kg of permanent magnet
 volume = Area x Stack length.

2.3.2 Mesh, magnetic and properties setting

The steps, end time and division are set in the step control part while the stack length is set in the full model conversion. The steps, end time, division and stack length are set to 37, 0.012s, 36 and 70 mm, respectively. The end time, t_e of the motor is acquired based on Eq. 2.

$$t_e = \frac{1}{f_e} \quad \text{Eq. 2}$$

Where t_e corresponds to end time and f_e is electrical frequency. The formula specifies the electrical frequency in Eq.3.

$$f_e = N_r f_m \quad \text{Eq. 3}$$

Where f_e is known as the frequency of electricity. N_r is referred to as rotor machine number, while f_m is defined as motor frequency. Meanwhile, the motor frequency, f_m can be determined by Eq.4.

$$f_m = \frac{n}{60} \quad \text{Eq. 4}$$

In which f_m is motor frequency while n is referred to as motor velocity. The standard 60 seconds is equivalent to 1 minute.

2.3.3 Load test

The load test is simulated with the injection of the motor with specific current density J_A . Torque and flux relation at various J_A locations are evaluated to determine the torque variation pattern when the different current value is injected into the motor's FEM coil. All nine models are tested and simulated to determine the characteristics of torque, power and speed. During the load test, the strength of the armature current varies between 0 to 30 A_{rms}/mm². With this requirement, the current density maximum value is set based on Eq.5.

$$I_A = \frac{\sqrt{2} J_A \alpha_A \delta_A}{N_A} \quad \text{Eq. 5}$$

where

I_A = Inject current value of armature coil, A(peak)
 J_A = Armature coil current density, A_{rms}/mm²
 α_A = Armature coil filling factor (set to 0.5)
 δ_A = Armature coil slot area.
 N_A = Number of turns.

The current value determined for all nine designs which are based on Eq. 5 is shown in Table 2 by current injection of I_{peak} and I_{rms} to each current density, J_A by relation to the value of the slot area armature which is 298.7577 mm² and 42 as the number of turns from the design motor.

Table 2. Current injection of I_{peak} and I_{RMS} to its current density, J_A

Armature coil current density, J_A (A/mm ²)	Input current of armature coil, I_{peak} (A)	Input current of armature coil, I_{rms} (A)
0	0	0
5	17.05	24.11
10	34.09	48.21
15	51.14	72.32
20	68.18	96.42
25	85.23	120.53
30	102.27	144.64

Torque and power versus speed analysis was performed to observe the value of maximum torque, output power and motor speed (rpm). The motor's output power is determined by using Eq. 6 that is based on the torque versus speed curve.

$$P_o = \frac{2\pi N_M \tau}{60} \quad Eq. 6$$

where

N_M = Motor speed (rpm)

τ = Torque

2.3.4 Design methodology of optimization

In this particular section, design improvement is conducted in order to increase the performance of the machine in terms of average output torque and power. This includes by updating eight parameters as shown in Figure 4.

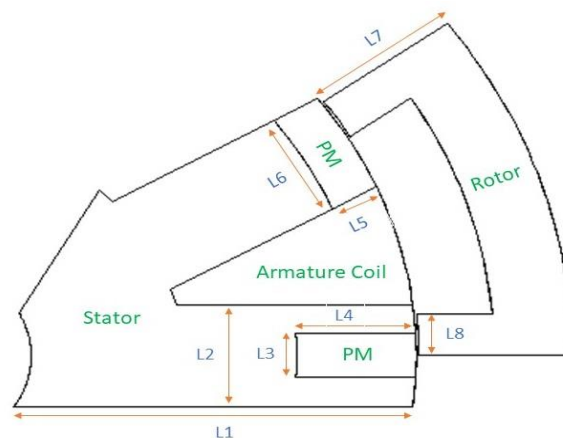


Figure 4 : Defined parameter L1 to L8 for design modification.

As the shape of initial design needs to be improved further, eight design parameters which are susceptible towards the advancement of machine performance are defined in permanent magnets, stator and rotor. The design parameters are split into three parts which are stator teeth length (L1) and stator tooth width (L2). The second part is the circumferential permanent magnet width (L3), circumferential permanent magnet depth (L4), radial permanent magnet width (L5) and radial permanent magnet depth (L6). Finally, the third part is the rotor pole length (L7) and the rotor pole width (L8). Regarding the area of armature coil and volume of permanent magnet, they are kept constant because when they are optimized, the average torque will be less than the initial design.

3. Results and Discussion

The proposed design of outer-rotor AlCiRaF PMFSM had been analyzed by using 2-dimensional finite element approach and result of both initial and optimized topologies are discussed in this section.

3.1 Results of no-load test

Data obtained in Figure 5 shows that this initial design has maximum value of magnetic density is 2.2114T and minimum value is 0.0002T. Thus giving interpretation that more room of flux can be generated in which causing machine to have higher possibility to be efficiently analyzed and utilized.

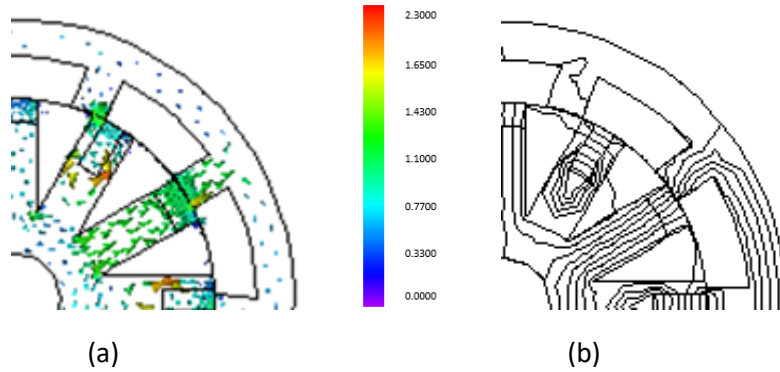


Figure 5: Initial topology (a) Electromagnetic flux contour (b) Flux linearity the

Figure 6 (a) illustrates the cogging torque graph for the initial and optimized design of proposed outer-rotor AlCiRaF PMFSM. The data shows that, initial 6S-10P AlCiRaF PMFSM has the peak to peak cogging torque value of 16.071 Nm. While optimized 6S-10P AlCiRaF PMFSM has the peak to peak cogging torque value of 14.394 Nm. Even though the value of cogging torque for optimized design is lower compared to initial design, it is still considered as high for cogging torque waveform. Therefore, design and settings should be modified in order for the waveform to meet the condition.

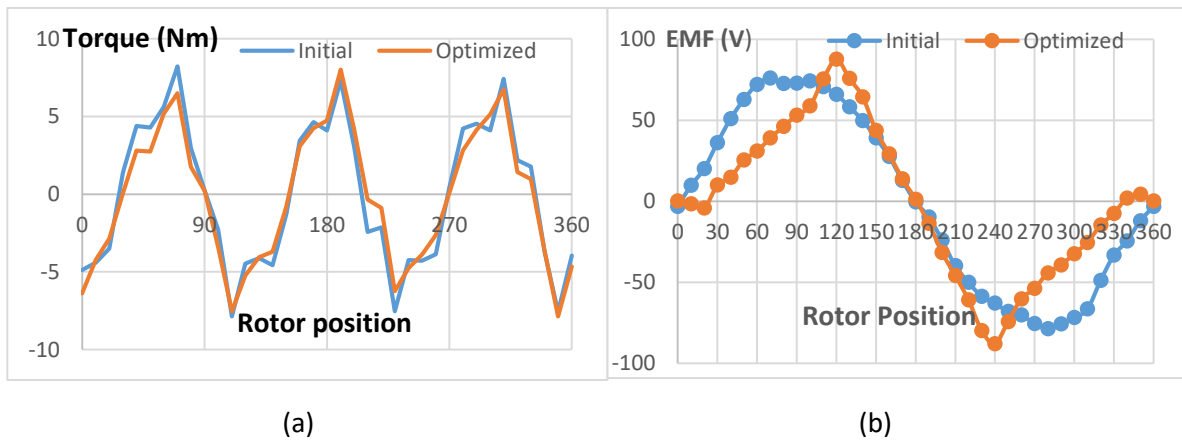


Figure 6: No-load initial and optimized graph (a) Cogging torque (b) Induced voltage

Meanwhile, Figure 6(b) shows the graph for back electromotive force (emf) of initial and optimized outer-rotor AlCiRaF PMFSM. Data shows that initial design has the maximum value of 76.032 V at angle of 70° while optimized design has the maximum value of 87.635 V at angle 120°. The configuration of waveform computed by optimized design is more favorable as it embraces the sinusoidal waveform.

3.2 Results of load test

Figure 7 (a) and (b) display the comparison between armature flux linkage for the initial and the optimized design at U phase for various armature current densities, J_A . J_A is analyzed as well in order to verify the flux characteristics.

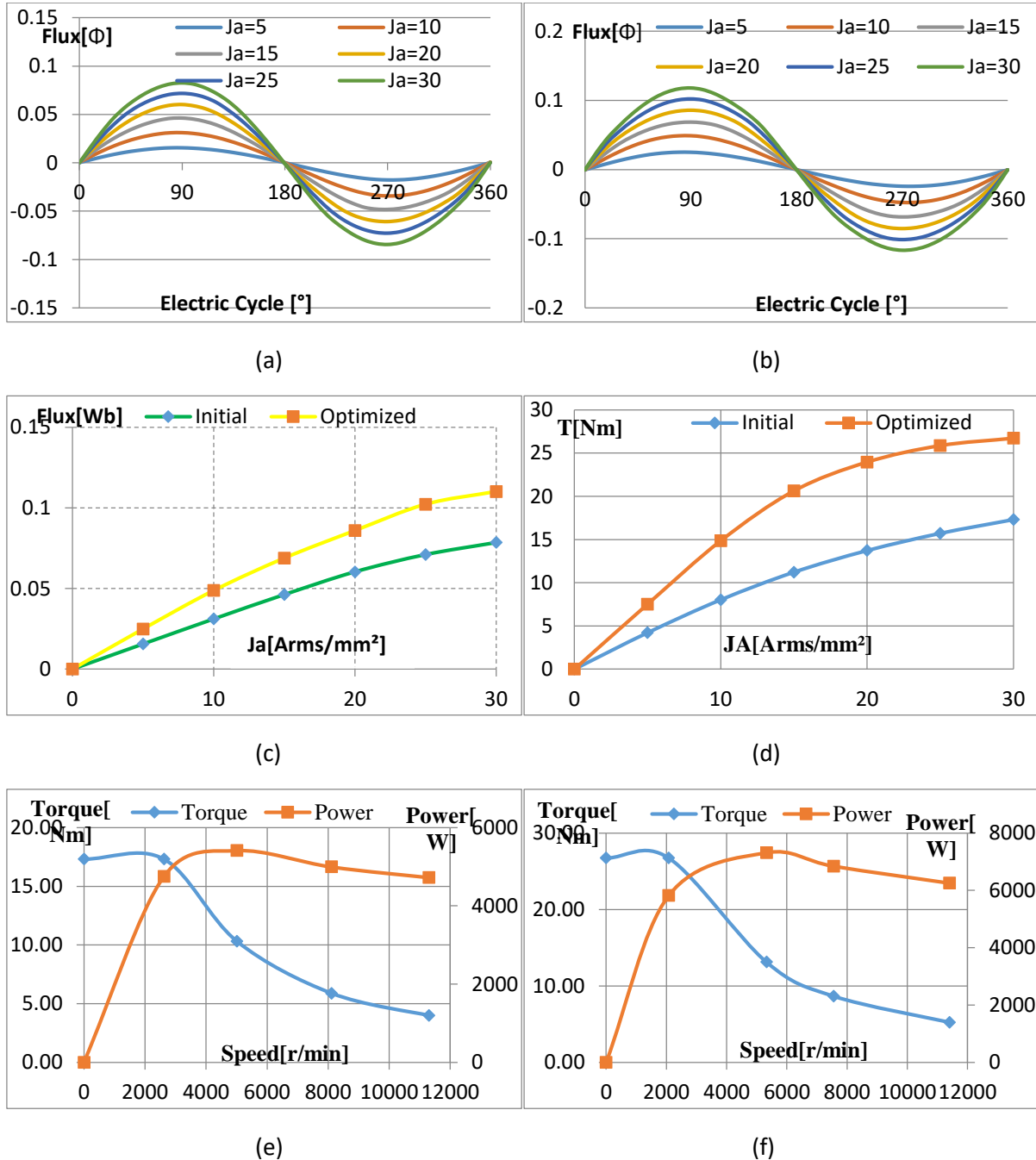


Figure 7: Initial and optimized graph under load test (a) Initial design (b) Optimized design (c) Maximum flux at various J_A for initial and optimized design (d) Initial and optimized torque at various J_A (e) Initial torque and power vs speed (f) Optimized torque and power vs speed

On the other hand, Figure 7(c) displays the comparison between maximum U phase flux at various J_A for initial and optimized design outer-rotor AlCiRaF PMFSM. It is obvious that the optimized design has the higher flux at all the J_A from 5 up to 30 Arms/mm². For optimized design, at $J_A = 30$ Arms/mm², the value of flux is 0.1101 Wb while for the initial design, at $J_A = 30$ Arms/mm², the value of

flux is 0.0785 Wb. Figure 7 (d) highlights the torque versus armature coil current densities, J_A , for initial and optimized design outer rotor AlCiRaF PMFSM. As can be observed, the torque of motor for optimized design is higher compared to initial design. The maximum torque obtained for initial design at armature coil current density, J_A of 30 A_{rms}/mm^2 is approximately 17.314 Nm and the minimum torque obtained for optimized design at armature coil current density, J_A of 5 A_{rms}/mm^2 is approximately 4.219Nm. The maximum torque obtained for optimized design at armature coil current density, J_A of 30 A_{rms}/mm^2 is approximately 26.726 Nm and the minimum torque obtained for optimized design at armature coil current density, J_A of 5 A_{rms}/mm^2 is approximately 7.526 Nm. Therefore, it could be predicted that the torque of optimized design has increased by 65 %. The torque and power versus speed characteristics of the initial and optimized design outer-rotor AlCiRaF PMFSM are illustrated in figure 7(e) and (f). Figure 7 (e) demonstrates the initial design where it has the maximum power of 5413 W at the 5014 r/min. While figure 7 (f) demonstrates the optimized design where it has the maximum power of 7312 W at the speed of 5324 r/min. From this, it could be seen that the power has increased almost 74 % at the approximate same range of r/min.

4. Conclusion

An advanced 6S-10P outer-rotor AlCiRaF PMFSM structure was proposed in this study. This work is divided into three parts which are initial design validation and analysis, optimization and comparison between initial and optimized design. In the beginning, initial design of 6S-10P outer-rotor AlCiRaF PMFSM has been validated and analyzed using JMAG Designer Version 16.1. After succeed validating, coil test analyzes are carried out to examine the design operating principles. The performance has been tested with no load and load condition. Next, optimization takes place where the main objective is to increase the torque. After the optimization process completes, optimized 6S-10P outer rotor AlCiRaF PMFSM achieved a torque increment from 17.314 Nm to 26.726 Nm which makes about 65 % increment. Besides that, cogging torque has decreased slightly from 16.071 Nm to 14.394 Nm which is about 10 % decrement. Finally, power has increased from 5413 W to 7312 W which makes about 74 % increment.

Acknowledgement

The authors would like to thank the Faculty of Electrical and Electronic Engineering, Universiti Tun Hussein Onn Malaysia for its support.

References

- [1] E. Hoang, A. H. Ben-Ahmed, and J. Lucidarne: "Switching flux permanent magnet polyphased synchronous machines," 7th Eur. Conf. Power Electronics and Applications, 3, 903–908, 1997.
- [2] M. Ehsani, Y. Gao, and J. M. Miller: "Hybrid electric vehicles: architecture and motor drives", Proc. IEEE, Vol. 95, No. 4, pp.719– 728, Apr 2011
- [3] M. Jenal, S. A. Hamzah, F. Khan, H. A. Soomro, and E. Sulaiman, "Performance investigations of flux switching machines for light weight electric vehicles," IEEE Conf. Energy Conversion, CENCON 2015, pp. 78–83, 2016.
- [4] Sulaiman, E.; Khan, F.; Ahmad, M.Z.; Jenal, M.; Zulkifli, S.A.; Bakar, A.A., "Investigation of field excitation switched flux motor with segmental rotor," 2013 IEEE Conference on Clean Energy and Technology (CEAT), pp.317-322, 2013
- [5] M. Jenal, E. Sulaiman, F. Khan and M. Z. Ahmad, "2D-FEA based design study of salient rotor three-phase permanent magnet flux switching machine with concentrated winding", Applied Mechanics and Materials, 785, pp 274-279, 2015.

- [6] H. Ali, E. bin Sulaiman, M. Jenal and M. F. Omar, "Three phase segmental rotor hybrid excitation flux switching motors for various applications," in Proc. 2015 IEEE Student Conference on Research and Development (SCORED), Kuala Lumpur, pp. 373-377, 2015.
- [7] Wu, Z. Z., and Z. Q. Zhu. "Analysis of magnetic gearing effect in partitioned stator switched flux PM machines." IEEE Transactions on Energy Conversion 31.4 (2016): 1239-1249. 2016.
- [8] M. Z. Ahmad, E. Sulaiman, M. Jenal, W. M. Utomo, S. A. Zulkifli, A. A Bakar, "Design Investigation of Three Phase HEFSM with Outer-Rotor Configuration" IEEE Conf. on Clean Energy & Technology, 18-20 Nov 2013.
- [9] Othman, S. M. N. S., et al. "Initial Design of 12s-10p and 12s-14p with Outer-Rotor Field-Excitation Flux Switching Machine." 2nd Power and Energy Conversion Symposium. 2014.
- [10] Y. Wang, M. J. Jin, J. X. Shen, W. Z. Fei, and P. C. K. Luk, "An outer-rotor flux-switching permanent magnet machine for traction applications," 2010 IEEE Energy Convers. Congr. Expo. ECCE 2010 - Proc., pp. 1723–1730, 2010.
- [11] W. Fei, P. C. K. Luk, J. X. Shen, Y. Wang, and M. Jin, "A novel permanent-magnet flux switching machine with an outer-rotor configuration for in-wheel light traction applications," IEEE Trans. Ind. Appl., vol. 48, no. 5, pp. 1496–1506, 2012
- [12] Enwelum I. Mbadiwe, Erwan Bin Sulaiman, "Design and optimization of outer-rotor permanent magnet flux switching motor using transverse segmental rotor shape for automotive applications:," Ain Shams Engineering Journal, pp. 1-10 2020.